



Published in final edited form as:

Chem Commun (Camb). 2019 May 25; 55(42): 5962–5965. doi:10.1039/c9cc02492a.

Phosphinate-containing rhodol and fluorescein scaffolds for the development of bioprobes†

Yuan Fang^a, Gillian N. Good^{a,b}, Xinqi Zhou^a, and Cliff I. Stains^{a,c,d}

^aDepartment of Chemistry, University of Nebraska-Lincoln, Lincoln, NE 68588, USA.

^bDepartment of Chemistry, Millersville University, Millersville, Pennsylvania 17551, USA

^cNebraska Center for Integrated Biomolecular Communication, University of Nebraska-Lincoln, Lincoln, NE 68588, USA

^dCancer Genes and Molecular Regulation Program, Fred & Pamela Buffet Cancer Center, University of Nebraska Medical Center, Omaha, NE 68198, USA

Abstract

A series of phosphinate-containing rhodol and fluorescein dyes are disclosed. These new fluorophores increase the color palette of phosphinate-based xanthenes in the far-red spectral region. The new chemical functionality of these scaffolds is leveraged to produce a sensitive, no-wash imaging probe for cellular esterase activity. The reported phosphinate-containing dyes provide platforms for the further development of imaging probes and self-reporting delivery vehicles.

Small molecule-based fluorescent probes represent attractive alternatives to fluorescent proteins for microscopy studies.^{1–3} Nonetheless, there is a need for the further development of red-shifted, photostable probes in order to enable the further development of robust bioprobes for imaging experiments. Towards this goal, recent efforts have focused on the introduction of heteroatoms into the bridging position of xanthene scaffolds.^{4–18} Our lab's approach to this problem involves replacement of the bridging oxygen atom in the rhodamine scaffold with a phosphinate functionality (Fig. 1).¹⁹ The resulting Nebraska Red (**NR**) fluorophores retain the brightness and photostability of the rhodamine scaffold, while displaying >110 nm shifts in excitation and emission. Furthermore, the unique chemistry of the phosphinate functional group allows for the construction of new enzymatic probes,²⁰ self-reporting small molecule delivery platforms,¹⁹ and provides inspiration for the development of new approaches for obtaining ratiometric probes.²¹ Building upon this, we sought to further increase the chemical functionality of **NR** dyes, through the synthesis and evaluation of rhodol- and fluorescein-based **NR** derivatives (Fig. 1). Importantly the phenol group present in these rhodol and fluorescein dyes provides a new chemical handle that can

†Electronic supplementary information (ESI) available: Experimental details, synthesis and characterization of new compounds, and supplementary figures. See DOI: 10.1039/c9cc02492a

Conflicts of interest

The authors declare no conflicts of interest.

be leveraged to construct sensitive, red-shifted enzyme-activated probes for cellular imaging studies.^{22–25}

Towards this goal, we first investigated synthetic routes capable of efficiently yielding rhodol and fluorescein **NR** derivatives. When compared to the synthesis of classical rhodamine dyes, insertion of phosphorous at the bridging position decreases the yield of the resulting fluorophore.^{9,19,26} Additional synthetic challenges arise in the case of fluorescein (due to the increased electron withdrawing capacity of the phenol group)¹⁰ and rhodol (due to the need to construct an asymmetric structure).^{27,28} During our investigation of different synthetic routes, the Yamaguchi group reported the direct conversion of phosphine oxide-containing rhodamines to rhodol and fluorescein *via* a hydrolytic deamination reaction under basic conditions (pH > 10).²⁹ As an initial examination of this route in the context of **NR** dyes, we incubated **NR700**, a phosphinate ester-based tetramethylrhodamine derivative, with 0.1 M NaOH. After 3 h the products of the reaction were purified by HPLC, yielding the hydrolysis product (**NR666**) and the corresponding rhodol product (**NR630**, Fig. S1 and Scheme S1, ESI†). Upon incubation of **NR700** with a 1 M solution of NaOH, instead of conversion to fluorescein we observed a rapid decrease in the color of the solution. This is likely due to attack at the C-9 position of the fluorophore as observed previously (Scheme S1, ESI†).²⁹ In support of this hypothesis, we observed a restoration of the solution's color upon addition of 2 M HCl. Nonetheless, we were very encouraged by the potential of this route to afford rhodol and fluorescein **NR** derivatives.

In order to protect the C-9 position from nucleophilic attack, we adopted previous strategies for introduction of bulky groups into xanthenes,^{29,30} incorporating dimethyl or dimethoxy groups at the C-2' and C-6' of our **NR** dyes (Fig. 1). Our previously reported route to **NR** rhodamine analogues, relied on the condensation of 3-bromo-*N,N*-dimethylaniline with benzaldehydes^{19,21} or the use of a xanthone precursor.^{10,12,19,31} However, as mentioned above, these routes result in relatively low yields of the target fluorophores. Building upon a previously described route for phosphine oxide fluorophores, we found that yields of **NR** rhodamines could be significantly increased by first treating 3-bromo-*N,N*-dimethylaniline with *sec*-butyllithium and exposing the resulting lithiated reagent to ethyl dichlorophosphite.²⁶ Subsequent oxidation with a 50% H₂O₂ solution yielded the phosphinate-bridged intermediate (**2**, Scheme 1a). A subsequent Vilsmeier–Haack reaction was used to generate the key intermediate **3**. Reaction of **3** with the appropriate lithiated 2,6-disubstituted phenyl reagents (dimethyl or dimethoxy) generated the corresponding secondary alcohol, which was directly treated with 2 M HCl under reflux overnight. Finally, *p*-chloranil was used to generate the **NR** rhodamine analogues containing bulky substituents proximal to the C-9 position. Compared to our previously reported routes,¹⁹ the newly developed intermediate **3** is accessible in relatively higher yields, leading to a 4-fold increase in the yield of **NR** rhodamines.

With the **NR** rhodamine analogues in-hand, we reassessed the ability to directly generate rhodol and fluorescein derivatives upon treatment with NaOH. Upon exposure to 0.1 M

†Electronic supplementary information (ESI) available: Experimental details, synthesis and characterization of new compounds, and supplementary figures. See DOI: [10.1039/c9cc02492a](https://doi.org/10.1039/c9cc02492a)

NaOH, the color of the solution quickly changed from green to purple, indicating the generation of **NR** rhodol (Scheme 1b). Monitoring by HPLC indicated that the reaction was complete after 4 h. As expected, the generation of **NR** fluorescein required a longer reaction time (3 days) and a higher concentration of base (1 M).²⁹ After purification by HPLC, the structures of all six **NR** derivatives were confirmed by NMR and mass spectrometry (see ESI[†]).

The photophysical properties of the **NR** rhodamine, rhodol, and fluorescein derivatives were assessed in PBS (10 mM, pH = 7.4) (Fig. 2a–c). The **NR** rhodamine derivatives showed the longest absorption and emission wavelengths, similar to our previously reported analogues.¹⁹ However, the **NR** rhodol and **NR** fluorescein derivatives displayed 35 and 70 nm blue-shifts, respectively relative to **NR** rhodamine. Comparison to the spectral properties of Tokyo Green,³² containing oxygen at the bridging position, indicated that introduction of the phosphinate in **NR** fluorescein resulted in a 109 nm red-shift. Among the **NR** family members, the dimethoxy analogues were slightly red-shifted compared to their dimethyl counterparts, while the dimethyl **NR** analogues displayed relatively higher brightness ($\epsilon \times \phi$) with the fluorescein dimethyl derivative (**NR**₆₀₀) displaying the overall the highest brightness. These **NR** dyes displayed blue-shifted excitation and emission maxima as well as increased brightness compared to previously reported phosphine oxide-based fluorophores (Table S1, ESI[†]).^{10,29}

Next, we investigated the equilibrium between protonated and deprotonated forms of the rhodol and fluorescein derivatives. Absorption of the **NR** rhodol and **NR** fluorescein dyes at varying pHs was recorded (Fig. S2, ESI[†]). From this data, the **NR** rhodol derivatives exhibited a pK_a of ~5.2 while the pK_a s for the **NR** fluorescein derivatives was ~6.7. Last, the photostability of **NR** family members was compared to Cy 5.5 using continuous irradiation for 1 h (Fig. 2d). Gratifyingly, all six **NR** dyes showed virtually no evidence of photobleaching, compared to a 50% decrease in Cy 5.5 fluorescence under the same conditions. Thus, these new **NR** derivatives provide a robust, tuneable palette of fluorescent reagents with emissions ranging from the far-red to near-infrared (NIR) region (Fig. 2e).

To highlight to utility of these new **NR** family members, we sought to develop a sensitive bioprobe for imaging enzymatic activity. For this application, we chose the dimethyl phosphinate-based fluorescein **NR**₆₀₀, due to its relative brightness. Importantly, previous work has clearly demonstrated the utility of acetoxymethyl (AM) ether groups for masking phenol functionalities within fluorophores.^{23–25,33} The resulting AM-protected probes display low background fluorescence, high chemical stability, and are readily cleaved by cellular esterases producing a turn-on fluorescent probe for esterase activity. Based on our previous results, we also anticipated that the negatively charged phosphinate of **NR**₆₀₀ would prevent the fluorophore from entering cells.¹⁹ Thus, we envisioned a diAM-protected version of **NR**₆₀₀, termed **diAM-NR**₆₀₀ (Fig. 3a). To examine the chemical stability of **diAM-NR**₆₀₀, an *in vitro* assay was conducted by monitoring the fluorescence generated by **diAM-NR**₆₀₀ over a period of 1 h (Fig. 3b). In the presence of pig liver esterase (PLE) we observed a clear, 13.8-fold increase in fluorescence that stabilized after 10 min. However, in the presence of PBS alone virtually no increase in fluorescence was observed. Moreover,

exposure to BSA or cell culture media containing 10% FBS produced relatively low background fluorescent signal (2.2- and 2.9-fold respectively). These data clearly indicate that **diAM-NR₆₀₀** can act as an esterase substrate, forming **NR₆₀₀** as a fluorescent product.

To interrogate the ability of **diAM-NR₆₀₀** to act as a no wash probe for cellular esterase activity, HeLa cells were incubated with the esterase probe and Cell Tracker Green CMFDA, in order to verify localization. Cells were then imaged, without washing, using confocal microscopy (Fig. 4a). Indeed, the formation of **NR₆₀₀** in the cytosol could clearly be observed within cells (Fig. S3a, ESI[†]), yielding a 10-fold increase in signal over background (Fig. 4b). Similar signal to noise was obtained in HeLa cells that were washed prior to imaging (Fig. S3b, ESI[†]). In addition, formation of **NR₆₀₀** was also observed in the cytosol of NIH-3T3 and RAW 264.7 cells, indicating the generality of **diAM-NR₆₀₀** (Fig. S4 and S5, ESI[†]). Decreased nuclear localization of **NR₆₀₀** was consistently observed relative to Cell Tracker Green CMFDA (a fluorescein derivative), indicating a potential difference in the nuclear accumulation of these dyes. Toxicity assays also clearly demonstrated that **diAM-NR₆₀₀** was not toxic at concentrations up to 10 mM (Fig. S6, ESI[†]). These experiments verify the ability of **diAM-NR₆₀₀** to act as a far-red emitting, no-wash probe for cellular esterase activity.

In summary, we have broadened the color palette of our **NR** dyes to include rhodol and fluorescein derivatives. The resulting **NR** rhodol and fluorescein dyes display significantly red-shifted fluorescence relative to their oxygen analogues and display increased photostability compared to commonly used labels such as Cy 5.5. The new chemical functionality afforded by these scaffolds enabled the development of a red-shifted, no-wash probe for cellular esterase activity. Current efforts in our lab are focused on lowering the pK_a of the **NR** fluorescein series to further increase the brightness at physiological pH. These new **NR** dye scaffolds also provide the starting point for the development of additional probes for enzymatic activity,³⁴ reagents for advanced imaging experiments,^{35–37} and self-reporting delivery reagents.¹⁹

We gratefully acknowledge the Morrison Microscopy Core Research Facility and Prof. Christian Elowsky for assistance with confocal fluorescence microscopy as well as Prof. Edward Harris for use of cell culture equipment. We also thank the Research Instrumentation/NMR facility and the Nebraska Center for Mass Spectrometry for assistance with characterization of new compounds. This work was funded by the NIH (R35GM119751), NSF (CHE-1757957), and the University of Nebraska-Lincoln. The content of this work is solely the responsibility of the authors and does not necessarily represent the official views of the NIH.

Supplementary Material

Refer to Web version on PubMed Central for supplementary material.

Notes and references

1. Lavis LD and Raines RT, ACS Chem. Biol, 2008, 3, 142–155. [PubMed: 18355003]
2. Lavis LD and Raines RT, ACS Chem. Biol, 2014, 9, 855–866. [PubMed: 24579725]

3. Lavis LD, *Biochemistry*, 2017, 56, 5165–5170. [PubMed: 28704030]
4. Koide Y, Urano Y, Hanaoka K, Terai T and Nagano T, *ACS Chem. Biol.*, 2011, 6, 600–608. [PubMed: 21375253]
5. Egawa T, Koide Y, Hanaoka K, Komatsu T, Terai T and Nagano T, *Chem. Commun.*, 2011, 47, 4162–4164.
6. Koide Y, Urano Y, Hanaoka K, Piao W, Kusakabe M, Saito N, Terai T, Okabe T and Nagano T, *J. Am. Chem. Soc.*, 2012, 134, 5029–5031. [PubMed: 22390359]
7. Koide Y, Kawaguchi M, Urano Y, Hanaoka K, Komatsu T, Abo M, Terai T and Nagano T, *Chem. Commun.*, 2012, 48, 3091–3093.
8. Grimm JB, Sung AJ, Legant WR, Hulamm P, Matlosz SM, Betzig E and Lavis LD, *ACS Chem. Biol.*, 2013, 8, 1303–1310. [PubMed: 23557713]
9. Chai X, Cui X, Wang B, Yang F, Cai Y, Wu Q and Wang T, *Chem. – Eur. J.*, 2015, 21, 16754–16758. [PubMed: 26420515]
10. Fukazawa A, Suda S, Taki M, Yamaguchi E, Grzybowski M, Sato Y, Higashiyama T and Yamaguchi S, *Chem. Commun.*, 2016, 52, 1120–1123.
11. Grimm JB, Gruber TD, Ortiz G, Brown TA and Lavis LD, *Bioconjugate Chem.*, 2016, 27, 474–480.
12. Liu J, Sun YQ, Zhang H, Shi H, Shi Y and Guo W, *ACS Appl. Mater. Interfaces*, 2016, 8, 22953–22962. [PubMed: 27548811]
13. Grimm JB, Brown TA, Tkachuk AN and Lavis LD, *ACS Cent. Sci.*, 2017, 3, 975–985. [PubMed: 28979939]
14. Piao W, Hanaoka K, Fujisawa T, Takeuchi S, Komatsu T, Ueno T, Terai T, Tahara T, Nagano T and Urano Y, *J. Am. Chem. Soc.*, 2017, 139, 13713–13719. [PubMed: 28872304]
15. Lutkus LV, Irving HE, Davies KS, Hill JE, Lohman JE, Eskew MW, Detty MR and McCormick TM, *Organometallics*, 2017, 36, 2588–2596.
16. Hirayama T, Mukaimine A, Nishigaki K, Tsuboi H, Hirose S, Okuda K, Ebihara M and Nagasawa H, *Dalton Trans.*, 2017, 46, 15991–15995. [PubMed: 28983547]
17. Fischer C and Sparr C, *Angew. Chem., Int. Ed.*, 2018, 57, 2436–2440.
18. Deng F and Xu D, *Chin. Chem. Lett.*, DOI: 10.1016/j.ccl.2018.10.1012.
19. Zhou X, Lai R, Beck JR, Li H and Stains CI, *Chem. Commun.*, 2016, 52, 12290–12293.
20. Chai X, Xiao J, Li M, Wang C, An H, Li C, Li Y, Zhang D, Cui X and Wang T, *Chem. – Eur. J.*, 2018, 24, 14506–14512. [PubMed: 30019781]
21. Zhou X, Lesiak L, Lai R, Beck JR, Zhao J, Elowsky CG, Li H and Stains CI, *Angew. Chem., Int. Ed.*, 2017, 56, 4197–4200.
22. Lavis LD, Chao TY and Raines RT, *ACS Chem. Biol.*, 2006, 1, 252–260. [PubMed: 17163679]
23. Lavis LD, Chao TY and Raines RT, *Chem. Sci.*, 2011, 2, 521–530. [PubMed: 21394227]
24. Tian L, Yang Y, Wysocki LM, Arnold AC, Hu A, Ravichandran B, Sternson SM, Looger LL and Lavis LD, *Proc. Natl. Acad. Sci. U. S. A.*, 2012, 109, 4756–4761. [PubMed: 22411832]
25. Chyan W and Raines RT, *ACS Chem. Biol.*, 2018, 13, 1810–1823. [PubMed: 29924581]
26. Fukazawa A, Usaba J, Adler RA and Yamaguchi S, *Chem. Commun.*, 2017, 53, 8565–8568.
27. Sednev MV, Wurm CA, Belov VN and Hell SW, *Bioconjugate Chem.*, 2013, 24, 690–700.
28. Roth A, Li H, Anorma C and Chan J, *J. Am. Chem. Soc.*, 2015, 137, 10890–10893. [PubMed: 26305899]
29. Grzybowski M, Taki M and Yamaguchi S, *Chem. – Eur. J.*, 2017, 23, 13028–13032. [PubMed: 28748577]
30. Lei Z, Li X, Li Y, Luo X, Zhou M and Yang Y, *J. Org. Chem.*, 2015, 80, 11538–11543. [PubMed: 26523465]
31. Best QA, Sattenapally N, Dyer DJ, Scott CN and McCarroll ME, *J. Am. Chem. Soc.*, 2013, 135, 13365–13370. [PubMed: 23889259]
32. Urano Y, Kamiya M, Kanda K, Ueno T, Hirose K and Nagano T, *J. Am. Chem. Soc.*, 2005, 127, 4888–4894. [PubMed: 15796553]
33. Levine SR and Beatty KE, *Chem. Commun.*, 2016, 52, 1835–1838.
34. Casey GR and Stains CI, *Chem. – Eur. J.*, 2018, 24, 7810–7824. [PubMed: 29338103]

35. Martineau M, Somasundaram A, Grimm JB, Gruber TD, Choquet D, Taraska JW, Lavis LD and Perrais D, *Nat. Commun*, 2017, 8, 1412. [PubMed: 29123102]
36. Wang C, Taki M, Sato Y, Fukazawa A, Higashiyama T and Yamaguchi S, *J. Am. Chem. Soc*, 2017, 139, 10374–10381. [PubMed: 28741935]
37. Grzybowski M, Taki M, Senda K, Sato Y, Ariyoshi T, Okada Y, Kawakami R, Imamura T and Yamaguchi S, *Angew. Chem., Int. Ed*, 2018, 57, 10137–10141.

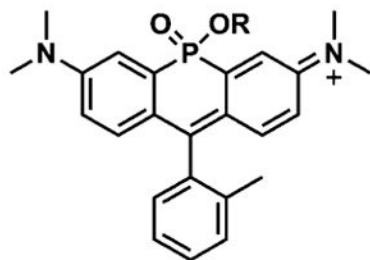
Author Manuscript

Author Manuscript

Author Manuscript

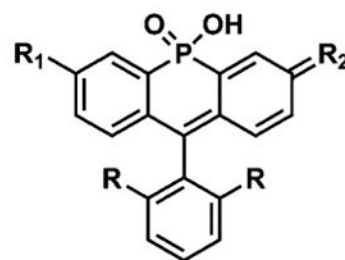
Author Manuscript

Previous work: Red-Shifted Rhodamines



NR₇₀₀ R = Et
 NR₆₆₆ R = H

This work: Expanded Xanthene Palette



R = OMe or Me
 NR Rhodamine: R₁ = NMe₂, R₂ = NMe₂⁺
 NR Rhodol: R₁ = NMe₂, R₂ = O
 NR Fluorescein: R₁ = OH, R₂ = O

Fig. 1.
 Structures of xanthene-based Nebraska Red family members.

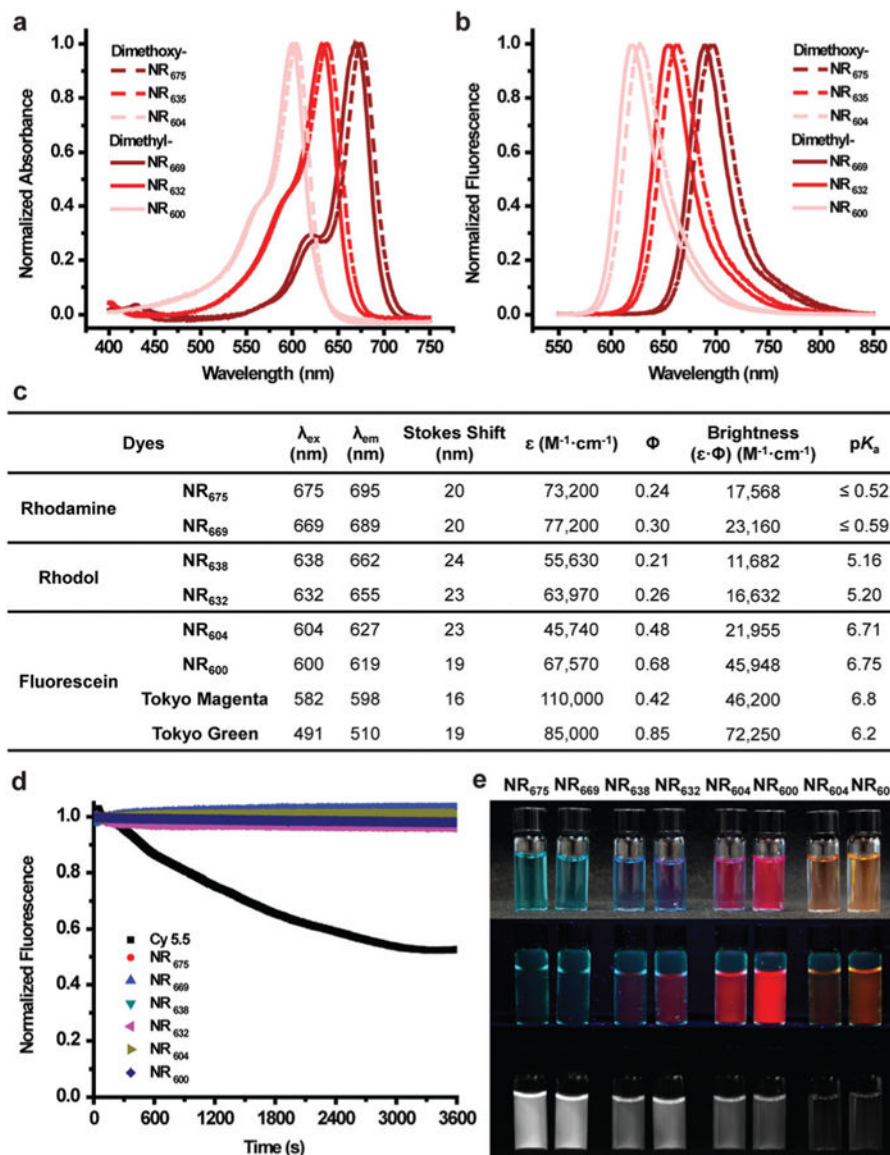


Fig. 2. Photophysical properties and pK_a s of NR family members. All experiments were conducted in PBS buffer (10 mM, pH = 7.4 containing 1% DMSO). (a) Normalized absorption spectra. (b) Normalized emission spectra. (c) Summary of optical parameters including previously reported values for Tokyo Magenta⁵ and Tokyo Green.³² (d) Photostability in comparison to Cy 5.5. (e) Images corresponding to each dye solution. From top to bottom: white-light image, fluorescent image under a UV lamp (254 nm), and a NIR image with a 680 nm filter. From left to right: NR₆₇₅, NR₆₆₉, NR₆₃₈, NR₆₃₂, NR₆₀₄, and NR₆₀₀ in PBS buffer as well as NR₆₀₄ and NR₆₀₀ in buffer at pH = 4.0.

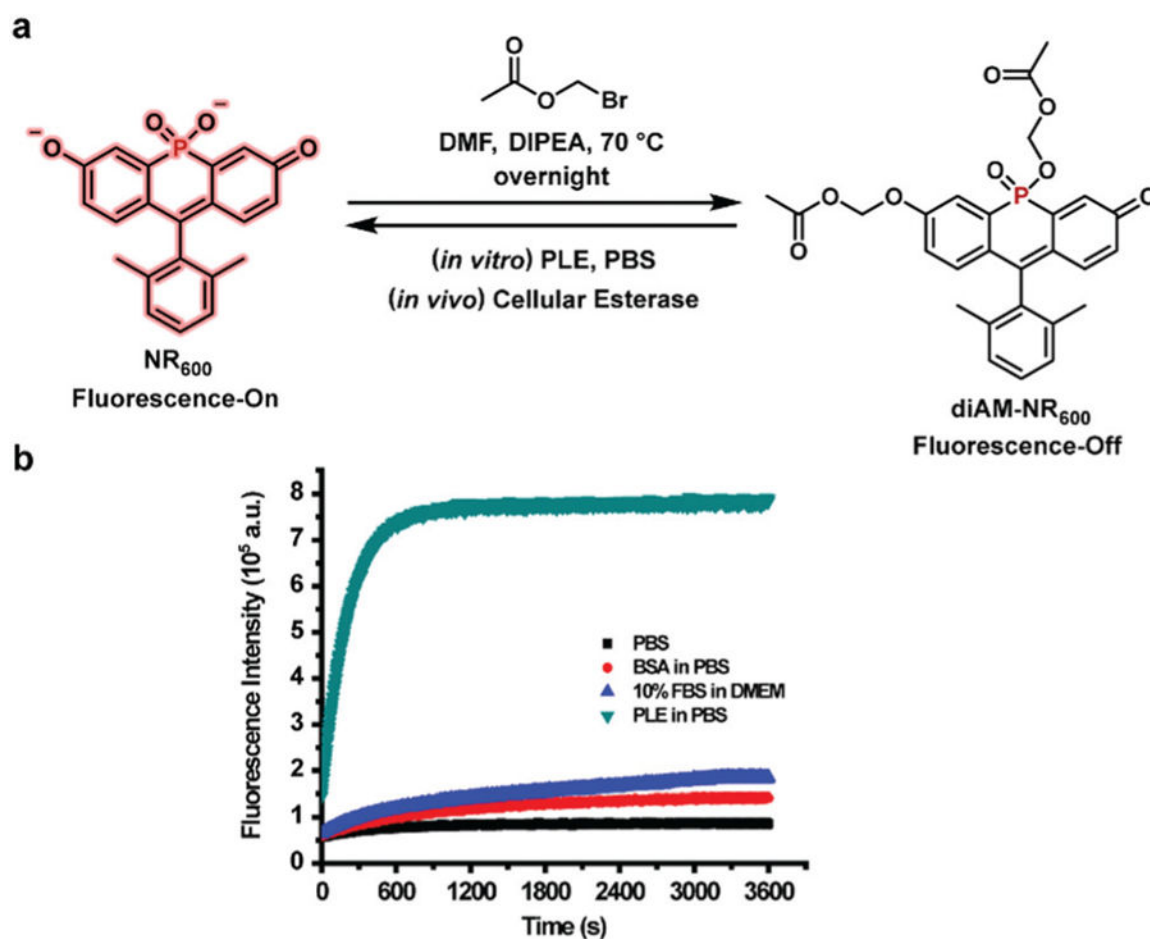


Fig. 3. (a) Synthesis of the esterase sensor **diAM-NR₆₀₀**. (b) *In vitro* stability of **diAM-NR₆₀₀** (5 μ M) in PBS (10 mM, pH = 7.4) alone or in the presence of BSA (0.2 units) or PLE (0.2 unit). The fluorescence of **diAM-NR₆₀₀** in cell culture media (DMEM with 10% FBS) is also shown. Fluorescence emission at 619 nm was monitored using excitation at 600 nm.

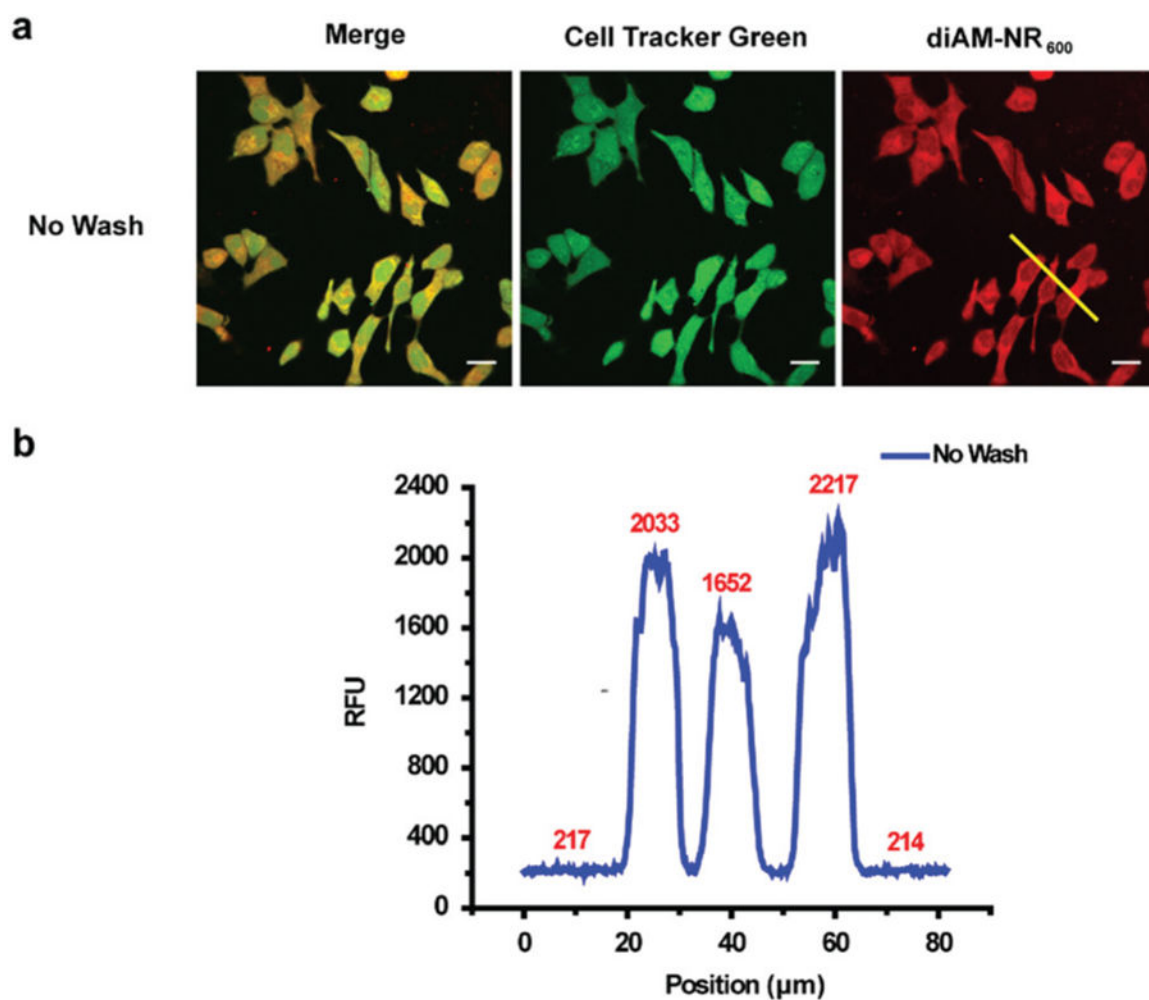
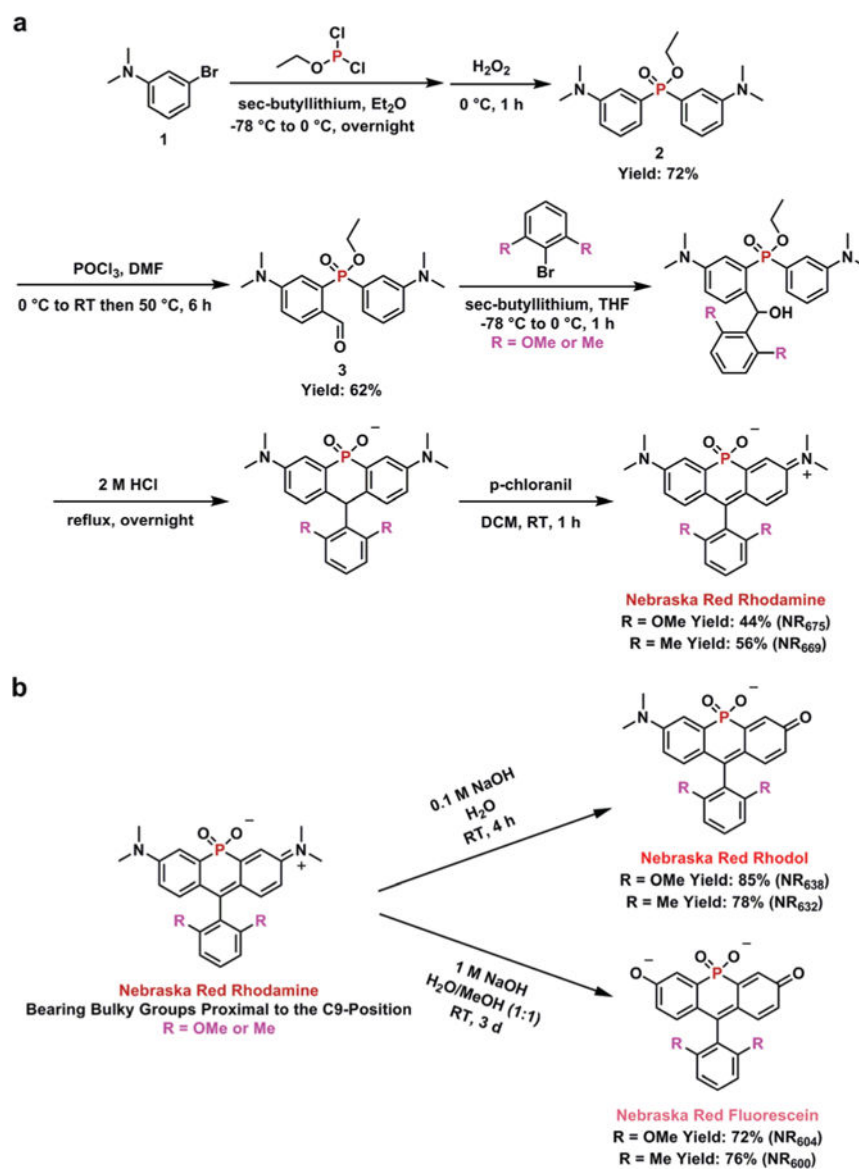


Fig. 4. (a) Confocal fluorescence microscopy imaging of HeLa cells incubated with 0.6 mM Cell Tracker Green CMFDA for 20 min followed by 0.6 μM diAM-NR₆₀₀ for 30 min (Scale bar: 20 μm). (b) Quantification of fluorescence intensity from panel a (yellow line in red channel).

**Scheme 1.**

(a) Synthesis of phosphinate-based NR rhodamine analogues. (b) Direct transformation of NR rhodamine to NR rhodol or NR fluorescein.